A High Reynolds Number Turbulent Boundary Layer with Regular 'Braille-Type' Roughness

Jason P. Monty, Min S. Chong, Romaine Mathis, Nicholas Hutchins, Ivan Marusic, and James J. Allen

Abstract A new high Reynolds number wind-tunnel facility at New Mexico State University (NMSU) was fitted with a roughened surface consisting of sheets of paper embossed by a Braille printer. The resulting roughness distribution was regular, three-dimensional and relatively sparse in the spanwise direction. Careful hot-wire studies show that the near-wall peak in turbulence intensity is reduced by the roughness, as expected. Comparisons with smooth-wall data indicate that turbulence is only affected by the roughness in the near-wall region, again as expected. However, analysis of the energy spectra showed an unexpected result: large-scale structures are significantly influenced by the roughness elements, despite the elements being $\sim$2 orders of magnitude smaller in size than these large-scale motions. This result excites the possibility of manipulating large-scale flow features with tiny protrusions.

1 Introduction

The effects of roughness on high Reynolds number turbulent flow forming over a solid boundary is of obvious practical importance, but will also aid in the ongoing pursuit of understanding the physics of wall-turbulence in general. The majority of research in this area has involved idealised, regular roughness. The aim is often to characterise roughness effects in terms of an 'equivalent sand-grain roughness', after the seminal work of Nikuradse [8]. To characterise a given roughness

J.P. Monty (✉), M.S. Chong, R. Mathis, N. Hutchins, and I. Marusic
Department of Mechanical Engineering, The University of Melbourne, Victoria 3010, Australia
e-mail: montyjp@unimelb.edu.au

J.J. Allen
Department of Mechanical Engineering, New Mexico State University, Las Cruces, NM 88003, USA

T.B. Nickels (ed.), *IUTAM Symposium on The Physics of Wall-Bounded Turbulent Flows on Rough Walls*, IUTAM Bookseries 22, DOI 10.1007/978-90-481-9631-9_10,

geometry requires both a parametric study of the important geometric characteristics (e.g. height, spacing) and measurements over a large range of Karman number – the Karman number, $Re_\tau = U_\tau \delta/\nu$, is a ratio of the boundary layer thickness to the viscous length scale, ν/U_τ; U_τ is the friction velocity ($= \sqrt{\tau_o/\rho}$, where ρ is the density and τ_o is the wall shear stress), δ is the boundary layer thickness and ν is the kinematic viscosity. Experimentally, this task is extremely difficult as facilities capable of the necessary Karman number range are rare and varying roughness parameters is a time, cost and labour intensive exercise. There are only limited examples of investigations that have overcome these obstacles, e.g. [1, 2, 10–12]. This presents the rough-wall turbulence researcher with a number of choices: either attempt a full parametric study in the vein of Schultz and Flack [11]; characterise limited roughness geometries with limited Reynolds number range; study practical roughness (e.g. [6]); or investigate in greater detail the flow field of roughness-affected wall-turbulence. The current work takes the latter course. Specifically, we aim here to investigate the structure of the high Reynolds number flow above a roughened wall using highly accurate hot-wire anemometry techniques. Single-point first- and second-order statistics will be shown along with energy spectra to highlight changes to structural properties of the flow by the roughness.

2 Experimental Apparatus

The highly ordered roughness surface was generated by a tractor-fed Braille embosser, allowing virtually unlimited length strips of roughness to be manufactured quickly. A characteristic segment of the Braille surface used in this study is shown in Fig. 1. The important features of this roughness type, with height $k = 0.4$ mm, are the regularity of the roughness and the sparsity in the spanwise direction.

Experiments were conducted in the NMSU high Reynolds number wind tunnel, having the desirable characteristics of an easily adjustable pressure gradient and low freestream turbulence intensity (less than 0.25%). The length of the 1.2 m × 1.2 m

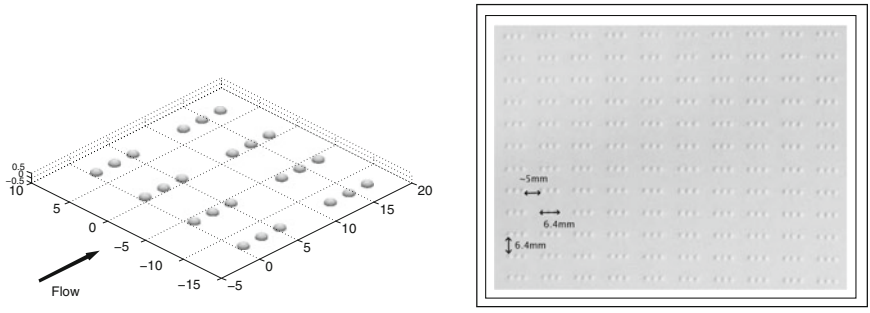

Fig. 1 Braille printed directional 'roughness' surface tested in NMSU tunnel (dimensions in mm). *Left*: schematic, scaled drawing. *Right*: photograph of the braille-embossed paper

working section is 15 m with a boundary layer thickness up to $\delta_{99} = 180$ mm. The freestream tunnel speed can reach 40 m/s giving a maximum Karman number of $Re_\tau = 12{,}000$ for the smooth-wall case. Normal hot-wire measurements were conducted with a custom-made hot-wire anemometer circuit. Wollaston wire was used for the sensing element, having exposed platinum of diameter between 1.5 – 5 μm and length-to-diameter ratio of at least 200. Recent work by Hutchins et al. [4] has shown that spatial resolution is a significant issue when measuring small-scale velocity fluctuations. They suggest that the non-dimensional sensing element length $l^+ = lU_\tau/\nu$ is the pertinent parameter for hot-wire anemometry. As such, considerable effort was imparted to ensure that $l^+ \approx 18$ was held constant for all experiments.

3 Results

Measurements were taken at four Karman numbers: $Re_\tau = 3{,}200$, 4,900, 6,850 and 10,000. Lower order statistics and a brief analysis of energy spectra are presented below. Considering the spanwise sparsity, it is important to state that all measurements shown were taken *between* elements in the spanwise direction, approximately 2.5 mm from the center of the nearest roughness element (in the scaled schematic of Fig. 1, this corresponds roughly to the coordinates −10 mm spanwise, +5 mm streamwise).

3.1 Mean Velocity and Turbulence Intensity

Firstly, the mean velocity data are shown with inner and outer scaling in Fig. 2. This statistic shows the expected roughness trends; that is, a vertical shift in the mean

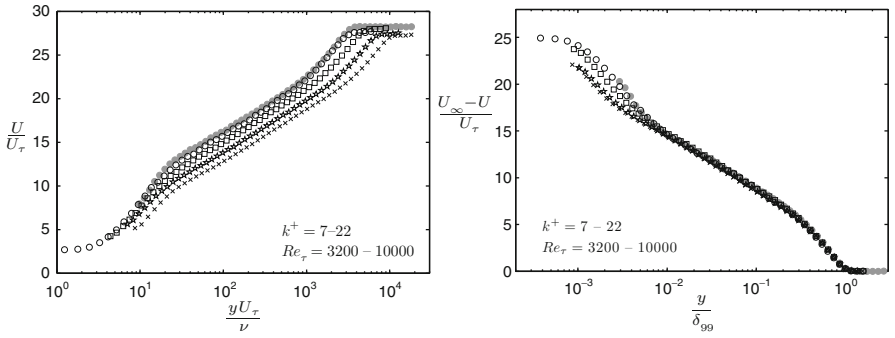

Fig. 2 Mean velocity profiles, *left figure* in inner scaling and *right figure* in defect form. *Grey circles* represent smooth-wall data from the Melbourne Tunnel. U_∞ is the freestream velocity

velocity with inner scaling. The method to determine the friction velocity, U_τ, was a somewhat subjective, but novel, method. First, U_τ was determined from a modified Clauser fit to the data [9]. However, the modified Clauser method is far from ideal, so an 'improvement' to the U_τ determined was achieved by assuming Townsend's similarity hypothesis to be true and determining the U_τ that best collapsed all of the mean velocity defect *and* turbulence intensity data in the outer region. Note that this process does not preferentially force collapse of the turbulence intensity or velocity defect, but rather finds the U_τ that best collapses both. It should also be noted that the process of enforcing outer-layer similarity only affected the Clauser calculated U_τ values by, at most, -7%(-1.45% on average across all Reynolds numbers). The authors are comfortable with this approach for two reasons: recent work (e.g., [2,5]) has shown that for three-dimensional roughness, outer-layer similarity is preserved; and, moreover, the conclusions of this study are independent of U_τ within the uncertainty of its determination using the process described here.

Turbulence intensity is shown in the two plots of Fig. 3. Again, the trends in this statistic with increasing Reynolds number and non-dimensional roughness height are clear and as expected: the logarithmic region displays an increasing turbulence intensity with Re_τ, while the inner region peak decreases. Importantly, the spatial resolution effects commonly responsible for decreased peak intensity are absent from this plot as the non-dimensional sensor length was kept constant. As such, the decreasing peak observed is due solely to roughness effects. In the right-hand graph of Fig. 3, the turbulence intensity for a single Reynolds number is compared with smooth wall data from the High Reynolds number Boundary Layer Wind Tunnel at the University of Melbourne (see [4] for further details). The agreement in the outer region is very good and there is a clear departure of the rough from the smooth at $y^+ \approx 200$ ($y/\delta_{99} \approx 0.03$) corresponding to $y \approx 13k$. Thus the roughness effect extends considerably further than the $5k$ criteria suggested by Flack et al. [3]. Once again, spatial resolution should not have a significant effect on this comparison as both experiments had similar sensor lengths of $l^+ = 18$ (rough) and $l^+ = 22$ (smooth).

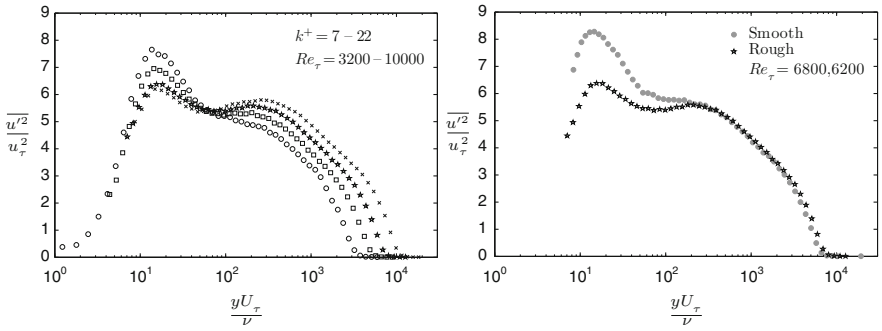

Fig. 3 Turbulence intensity profiles. *Left*: all rough-wall with matched l^+. *Right*: comparison between rough– ($l^+ = 18$, $k^+ = 15$) and smooth-wall ($l^+ = 22$) data at similar Re_τ

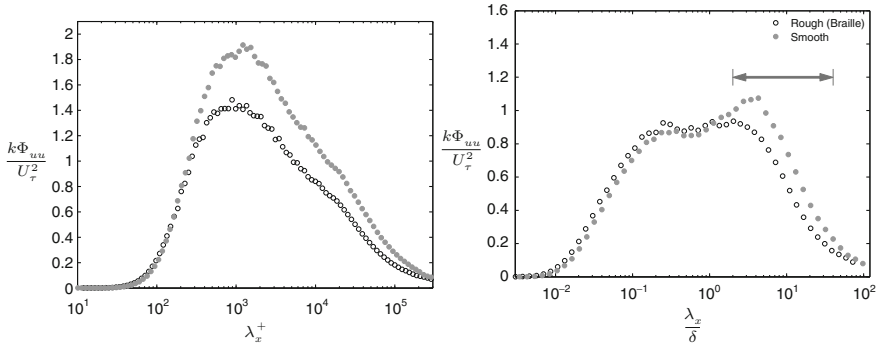

Fig. 4 Pre-multiplied spectra for rough and smooth cases at $yU_\tau/\nu = 100$. The *thick arrow* highlights the wavelengths where the two cases differ substantially

3.2 Energy Spectra

The energy spectra shown in Fig. 4 shows an unexpected result: when compared with the energy distribution over a smooth-wall (solid circles), the effect of the roughness is a reduction of the energy contribution from the largest scale eddies (in the region highlighted by the arrow in Fig. 4), even in the log region. These large eddies have length of $\sim 6\delta$ which corresponds to ~ 1 m in the NMSU tunnel. Furthermore, the smaller-scale structures appear unaffected by roughness in the log region. Analysis of spectra at all roughness-affected wall-normal locations (i.e., $y^+ < 200$, not shown here for brevity) shows the large-scale component of the velocity is modified throughout the log-region *and* right down to the wall.

This result suggests that it is possible to manipulate the largest energetic structures in wall-turbulence with tiny passive obtrusions. Considering the largest structures have height, $O(\delta)$ and the roughness elements are more than 3 orders of magnitude smaller ($\approx 0.002\delta$ in height), this is a remarkable result.

3.3 Amplitude Modulation

In a recent paper by Mathis et al. [7], the largest-scales in smooth-wall turbulence, $O(6\delta)$ in length, are shown to amplitude modulate the small-scales, $O(1000\nu/U_\tau)$, at high Reynolds number. The high Reynolds number is necessary to allow sufficient scale separation between the small and large scales. Here we perform a similar procedure, which is only briefly described, with full details available in [7]. First, at a given distance from the wall, a low-pass Fourier filter is applied to the velocity time-series to isolate the large-scale signal, termed u_L^+ as shown in Fig. 5. The cut-off frequency chosen was $\lambda_x^+ = 7300$, where $\lambda_x^+ = \lambda_x \nu/U_\tau$ is the non-dimensional streamwise wavelength. A high-pass filter is also applied separating the smaller-scales, termed u_S^+. Using a Hilbert transform procedure on the small-scale

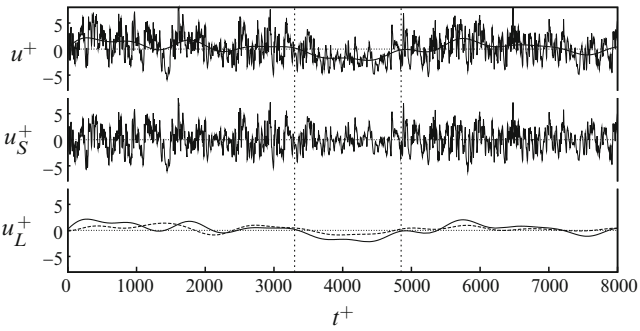

Fig. 5 Sample of streamwise velocity time-series at $y^+ = 15$: *top*, true velocity with overlaid large-scale component, u_L^+; *middle*, small-scale component, u_S^+; *bottom*, u_L^+ (*solid*) plotted with filtered envelope of u_S^+ (*dashed*) – note that the envelope has been shifted to have zero mean for comparison with u_L^+. *Vertical dotted lines* highlight a large, low-speed event

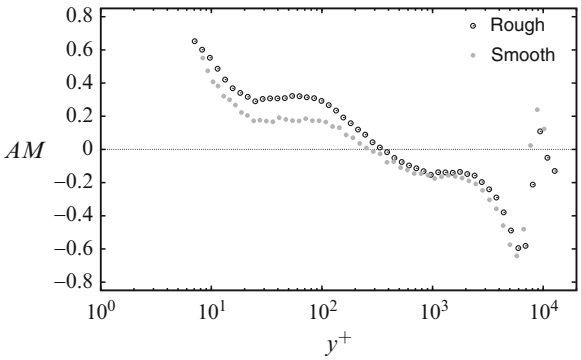

Fig. 6 Amplitude modulation coefficient for rough and smooth cases at $Re_\tau = 6{,}800$ and $Re_\tau = 6{,}200$ respectively

signal, u_S^+, provides the envelope of the small-scale signal. That envelope is then low-pass filtered with the same cut-off frequency given above. The correlation of the large-scale velocity trace, u_L^+ and the low-pass filtered envelope of u_S^+ provides a measure of the amplitude modulation of the small-scales by the large, termed AM. This procedure can be performed at each wall-normal location, giving $AM(y)$. The result of this analysis is shown in Fig. 6. The figure shows a similar distribution of amplitude modulation between smooth and rough walls, particularly in the outer region. Near the wall, however, there is a marked increase in amplitude modulation in the rough-wall case. This important result confirms that the structure of the flow around roughness elements at high Reynolds numbers will depend on the state of the large-scale events far from the wall, which are much larger than the roughness elements. This further indicates that care should be taken when constructing numerical or analytical models (based on observations such as separation from, and reattachment to, roughness elements) from low Reynolds number studies.

4 Conclusions

A careful experimental program in a high-quality boundary layer facility at NMSU has provided a unique database of high Reynolds number, high fidelity, streamwise velocity measurements over a sparse rough-wall. The lower-order statistics exhibited the expected trends and it has been shown that the amplitude modulation of large-scale structures on smaller-scales occurs in rough-walls in a similar way to that observed in smooth-wall flows. In fact, the amplitude modulation is stronger in the rough-wall flow compared with the smooth-wall below the logarithmic region. Finally, the very small roughness elements were seen to modify the large-scale structures in the zero-pressure-gradient turbulent boundary layer, and this may have implications for passive drag reduction or augmentation strategies.

References

1. J.J. Allen, M.A. Shockling, G.J. Kunkel, A.J. Smits, Turbulent flow in smooth and rough pipes. Phil. Trans. R. Soc. A **365**(1852), 699–714 (2007)
2. K.A. Flack, M.P. Schultz, T.A. Shapiro, Experimental support for townsend's reynolds number similarity hypothesis on rough walls. Phys. Fluids **17**, 035102 (2005)
3. K.A. Flack, M.P. Schultz, J.S. Connelly, Examination of a critical roughness height for outer layer similarity. Phys. Fluids **19**(9), 095104 (2007)
4. N. Hutchins, T.B. Nickels, I. Marusic, M.S. Chong, Hot-wire spatial resolution issues in wall-turbulence. J. Fluid Mech. **635**, 103–136 (2009)
5. J. Jimenéz, Turbulent flow over rough walls. Annu. Rev. Fluid Mech. **36**, 173–196 (2004)
6. L.I. Langelandsvik, G.J. Kunkel, A.J. Smits, Flow in a commercial steel pipe. J. Fluid Mech. **595**, 323–339 (2008)
7. R. Mathis, N. Hutchins, I. Marusic, Large-scale amplitude modulation of the small-scale structures in turbulent boundary layers. J. Fluid Mech. **628**, 311–337 (2009)
8. J. Nikuradse, Gesetzmassigkeiten der turbulenten stromung in glatten rohren. Forsch Auf Dem Gebiet des Ingenieurwesens **3**, 1–36 (1932)
9. A.E. Perry, J.D. Li, Experimental support for the attached-eddy hypothesis in zero-pressure-gradient turbulent boundary layers. J. Fluid Mech. **218**, 405–438 (1990)
10. H. Schlichting, Experimental investigation of the problem of surface roughness. Tech. Rep. 823, N. A. C. A. (1936)
11. M.P. Schultz, K.A. Flack, Turbulent boundary layers on a systematically varied rough wall. Phys. Fluids **21**(1), 015104 (2009)
12. M.A. Shockling, J.J. Allen, A.J. Smits, Roughness effects in turbulent pipe flow. J. Fluid Mech. **564**, 267–285 (2006)